Published in final edited form as:
J Mech Behav Biomed Mater. 2020 January ; 101: 103438. doi:10.1016/j.jmbbm.2019.103438.

An investigation of the effect of freezing storage on the biaxial mechanical properties of excised porcine tricuspid valve anterior leaflets

Grace Duginski[1], **Colton Ross**[1], **Devin Laurence**[1], **Cortland Johns**[1], **Chung-Hao Lee**[1,2]

[1]Biomechanics and Biomaterial Design Laboratory, School of Aerospace and Mechanical Engineering, The University of Oklahoma, Norman, OK 73019, USA

[2]Institute for Biomedical Engineering, Science and Technology, School of Aerospace and Mechanical Engineering, The University of Oklahoma, Norman, OK 73019, USA

Abstract

The atrioventricular heart valve (AHV) leaflets are critical to the facilitation of proper unidirectional blood flow through the heart. Previously, studies have been conducted to understand the tissue mechanics of the healthy AHV leaflets to inform the development of valve-specific computational models and replacement materials for use in diagnosing and treating valvular heart disease. Generally, these studies involved biaxial mechanical testing of the leaflet tissue specimens to extract relevant mechanical properties. Most of those researchers used freezing-based storage systems based on previous findings for other connective tissues such as aortic tissue or skin. However, there remains no study which specifically examines the effect of freezing storage on the characterized mechanical properties of the AHV leaflets. In this study, we aimed to address this gap in knowledge by performing biaxial mechanical characterizations of the tricuspid valve anterior leaflet (TVAL) tissue both before and after a 48-hour freezing period. Primary findings of this study include: (i) a statistically insignificant change in the tissue extensibilities, with the frozen tissues being slightly stiffer and more anisotropic than the fresh tissues; and (ii) minimal variation in the stress relaxation behaviors between the fresh and frozen tissues, with the frozen tissues demonstrating slightly lessened relaxation. The findings from this study suggested that freezing-based storage does not significantly impact the observed mechanical properties of one of the five AHV leaflets—the TVAL. The results from this study are useful for reaffirming the previous researchers' methodologies, as well as informing the tissue preservation methods of future investigations of AHV leaflet mechanics.

Keywords

the tricuspid valve; heart valve biomechanics; freezing storage effects; biaxial mechanical testing; stress relaxation

For correspondence: Chung-Hao Lee, Ph.D., Assistant Professor, School of Aerospace and Mechanical Engineering, Affiliated Faculty Member, Institute for Biomedical Engineering, Science, and Technology, The University of Oklahoma, 865 Asp Ave., Felgar Hall Rm. 219C, Norman OK 73019-3609, U.S.A., ch.lee@ou.edu, Tel: +1 405-325-4842.

Conflicts of Interest

The authors of this paper have no financial or personal relationships with other people or organizations that could inappropriately influence (bias) our work.

1. Introduction

The atrioventricular heart valves (AHVs) are critical in ensuring unidirectional flow of blood from the atria into the ventricles. The AHVs include the mitral valve (MV) and the tricuspid valve (TV), which are composed of soft tissue leaflets that facilitate proper blood flow by cyclically opening and closing throughout the cardiac cycle. When these valves fail to properly close, a regurgitant jet of blood occurs from the ventricles into the atria during systole, leading to insufficient blood in the ventricles and long-term health problems, such as an increased possibility of heart failure (Waller *et al.*, 1994; Waller *et al.*, 1995). Currently, research has been focused on the development of computational models and biomimetic materials for better understanding and treatment of valvular heart disease, such as valve regurgitation (Arzani and Mofrad, 2017; Kidane *et al.*, 2009; Kunzelman *et al.*, 1997; Lee *et al.*, 2015; Sun *et al.*, 2014). These studies were based on an understanding of the mechanical properties and behaviors of the heart valve leaflets. Determinations of the valve leaflets' properties are generally performed using a mechanical testing procedure, most primarily in the form of cyclic biaxial mechanical loading. Many of these prior studies of the AHV leaflets have utilized freezing-based storage systems to preserve the freshness of the leaflet tissues for extended periods of time (Eckert *et al.*, 2013; Grashow *et al.*, 2006; Huang *et al.*, 2012; Jett *et al.*, 2018; Laurence *et al.*, 2019; Liao *et al.*, 2007; Pham *et al.*, 2017; Pham and Sun, 2014; Pokutta-Paskaleva *et al.*, 2019; Stella *et al.*, 2007; Stella and Sacks, 2007) based on the findings in the previous literature for mechanical testing of other biological materials.

Previously, studies have had mixed or contradictory results regarding the effect of freezing on the mechanics of biological tissues. Some researchers have examined the efficacy of freezer storage for bone tissue (Kaye *et al.*, 2012; Linde and Sørensen, 1993; Pelker *et al.*, 1983) or cartilage (Changoor *et al.*, 2010), by performing mechanical characterizations of the structures both before and after freezing of the tissue. These researchers found that there was no significant change in the mechanical properties of these tissues influenced by freezing storage. Those researchers investigating tendons (Clavert *et al.*, 2001; Giannini *et al.*, 2008; Matthews and Ellis, 1968; Smith *et al.*, 1996), on the other hand, did find significant changes in the mechanical properties following freezing. Other researchers have looked specifically at soft biological tissues such as arteries (Delgadillo *et al.*, 2010; Venkatasubramanian *et al.*, 2006), aortic tissue (O'Leary *et al.*, 2014; Stemper *et al.*, 2007), skin (Foutz *et al.*, 1992) and liver (Santago *et al.*, 2009). Researchers analyzing freezing effects on soft tissues have mixed results, where some studies found no significant changes in the observed mechanical properties due to freezing (Delgadillo *et al.*, 2010; O'Leary *et al.*, 2014; Stemper *et al.*, 2007), while others observed notable changes in the tissue's mechanical properties, such as the elastic modulus or failure strain (Santago *et al.*, 2009; Venkatasubramanian *et al.*, 2006). Furthermore, the storage methods for the tissues vary greatly from study to study, including refrigeration at 4 °C, freezing at temperature levels ranging from −20 °C to −80 °C (or even as low as −196 °C), several freeze-thaw cycles or rates of freezing, and the use of liquid nitrogen.

To elaborate on these inter-study variations, for example, Delgadillo *et al.* used cryoprotective solutions when freezing arterial tissue, which may explain why they did not

observe a change in the tissue mechanical response as compared to Venkatasubramanian *et al.*, who observed a change in the elastic modulus using the same tissue type and storage temperature as Delgadillo *et al.* Stemper *et al.* noticed a change in mechanical response of porcine aortas due to refrigerator storage (4 °C) but not freezer storage (−20 °C or −80°C). Additionally, Santago *et al.* found a difference in failure strain for liver tissue, which they explained was due to the microstructure of the tissue. Santago *et al.* proposed that the liver tissue has a greater proportion of cells compared to other tissues, such as tendon, and that the cells sustained damage due to the freezer storage. The differences in the freezing storage methods or type of biological tissue may explain the variety of results from these researchers in the soft tissue biomechanics literature.

Although the effect of freezing on the mechanical properties of many other soft biological tissues has been investigated, there still exists a gap in literature on the freezing-induced effects on the observed mechanical properties of the atrioventricular heart valve leaflets. Previous researchers of the AHV leaflets employed a freezing-based storage system for their studies based on the assumption that results from studies of other soft biological tissues, such as arteries, skin or aortic tissue—analogous for the heart valve leaflets, *which may not necessarily be valid*. Therefore, our primary goal in this study is to fill this gap in knowledge by examining the effects of freezing-based storage on the characterized tissue mechanics of one of the five AHV leaflets—the tricuspid valve anterior leaflet (TVAL). This investigation was done by performing biaxial mechanical testing and stress relaxation testing of the selected AHV leaflet tissue specimens before and after freezer storage. Our findings in this study will provide helpful insight into the AHV leaflet-specific storage methods, which will be informative to the future use of freezing storage in AHV leaflet tissue experiments.

2. Methods

2.1 Tissue acquisition and preparation

Healthy, adult porcine hearts (80–140 kg, 1–1.5 years of age, a female-to-male ratio of 1:1, n=10) were obtained from a local USDA-approved slaughterhouse (Chickasha Meat Co., Chickasha, OK). Then, the tricuspid valve anterior leaflet was excised from the heart within 3 hours of animal death. The TVAL was selected due to its large size relative to the other TV leaflets (Rogers and Bolling, 2009). Once excised, the leaflet was sectioned into a 10 × 10 mm square (Fig. 1a), and the tissue's circumferential and radial directions noted by labelling the top-right corner of the square tissue specimen using a surgical pen. The tissue thickness was measured with digital calipers (Westward 1AAU4 – 0.01 mm resolution) three times per sectioned leaflet. The three thickness measurements were then averaged to account for regional variations in tissue thickness. The tissue specimen was then mounted to a commercial biaxial mechanical testing system (BioTester, CellScale, Canada) using five-tined BioRakes. The fresh tissue specimens were mounted with an effective edge length of 6.5–8.5 mm, and the frozen tissues were mounted with a smaller effective edge length of 6.0–7.0 mm. Next, using a surgical pen, four fiducial markers were applied in a square configuration in the middle third of the tissue for later digital image correlation (DIC) methods (cf. Section 2.3). The tissue was submerged in a phosphate-buffered saline (PBS)

solution bath heated to 37 °C to emulate the physiological conditions for the biaxial mechanical testing as described in the next subsection.

A range of edge lengths were used in this study due to limitations based on the retrievable sizes of the tissue specimens. Additionally, different effective edge lengths were used between the fresh and frozen tissue samples because the same tissues were used both before and after freezer storage (cf. Section 2.2) and overlapping holes from the previous BioRake mounting could result in tissue tearing during testing. Additionally, preliminary results of an investigation in our lab suggest that the various edge lengths employed have a negligible effect on the measured tissue mechanical properties.

2.2 Biaxial mechanical testing

To compare the mechanical response of the fresh tissue specimen to the response after freezer storage, a sequential testing procedure was performed: (1) biaxial mechanical testing of a fresh (control) specimen, (2) freezing of the tissue for 48 hours, and (3) thawing and biaxial mechanical testing of the previously-frozen tissue using the same protocols as in Step (1). First, for biaxial mechanical testing of the fresh TVAL tissue specimen, a 12-cycle preconditioning protocol was performed that stretched the tissue specimen to a targeted membrane tension of 75 N/m (Fig. 1b). Tissues were tested to a membrane tension of 75 N/m to emulate both the physiological loading and the stress-overloading conditions of the TVAL (Ayoub *et al.*, 2017; Khoiy and Amini, 2016; Pant *et al.*, 2018). After preconditioning, mechanical testing protocols were performed as developed in our prior work for the TVAL tissues (Jett et al., 2018) with some minor modifications. These modifications included reducing the number of repetitions from 10 cycles to 4 cycles for each loading ratio and reducing the number of loading ratios from T_{circ}:T_{rad}=1:1, 1:0.75, 0.75:1, 1:0.5, and 0.5:1 to T_{circ}:T_{rad}=1:1, 1:0.5, and 0.5:1 (Fig. 1b), where T_{circ} and T_{rad} are the applied membrane tensions in the tissue's circumferential and radial directions, respectively. Data was collected from the last unloading cycle of each protocol.

Next, a stress-relaxation protocol was performed during which the tissue was stretched to the displacement associated with the peak membrane tension, held at the same displacement for 15 minutes, and the force decrease over time monitored (Fig. 1b). Throughout the biaxial testing and stress-relaxation 1280×960 images were captured at a rate of 15 Hz using a CCD camera mounted to the biaxial tester. In the meantime, load cell force and tine displacement readings were recorded by the biaxial tester. All protocols were performed on both fresh and frozen tissues. For freezer storage, the fresh tissue samples at room temperature were placed in plastic containers immediately after testing, and the containers stored in the freezer of a standard refrigerator (Frigidaire FRT18L4JW7) at −14°C for two days before further biaxial mechanical testing.

2.3 Tissue stress-stretch analysis

For more details on the stress and stretch calculations, refer to our previous publication (Jett *et al.*, 2018). Briefly, the DIC function of the BioTesting system software was used to determine the time-dependent pixel coordinates of the four fiducial markers. These marker positions were then used to calculate the deformation gradient **F** using a four-node bilinear

finite element (Sacks, 2000; Tadmor *et al.*, 2012). Next, principal stretches in the circumferential and radial directions (λ_{circ} and λ_{rad}) were calculated by taking the square roots of the principal values of the Cauchy-Green deformation tensor $\mathbf{C}=\mathbf{F}^T\mathbf{F}$. Tissue stretches were calculated with respect to different deformation states, including the peak stretch (${}^{2}_{0}\lambda$), which was the tissue stretch at the peak membrane tension with respect to the mounted tissue configuration (Ω_0), the preconditioning stretch (${}^{1}_{0}\lambda$), defined as the tissue stretch observed at the end of the preconditioning protocol determined between configuration Ω_0 and the post-preconditioning configuration (Ω_1), and the mechanical stretch ${}^{2}_{1}\lambda$, which was the tissue stretch at the peak membrane tension with respect to configuration Ω_1. The tissue stretches can be related by ${}^{2}_{0}\lambda = {}^{2}_{1}\lambda {}^{1}_{0}\lambda$.

As for the tissue stress calculation, the membrane tensions in both tissue directions (T_{circ} and T_{rad}) were determined by dividing the load cell's force reading by the effective edge length of the tissue specimen. Other stress measures, such as the Cauchy stress $\boldsymbol{\sigma}$, the first Piola-Kirchhoff stress **P** and the second Piola-Kirchhoff (2^{nd}-PK) stress **S**, can be computed using the thickness t of the tissue specimen (Reddy, 2013; Tadmor *et al.*, 2012). In addition, we also calculated the low-tension modulus (E^{LT}), the high-tension elastic modulus (E^{HT}), the index of extensibility (λ^*), and the anisotropy index (AI), which are described in more detail in previous studies (May-Newman and Yin, 1995; Pham *et al.*, 2017; Wells *et al.*, 2012). As illustrated in Figure 1c, E^{LT} refers to the tangent modulus at the pre-transitional region, E^{HT} denotes the tangent modulus at the post-transitional region, λ^* is the stretch as the intercept of the extended line of the post-transitional tangent, and AI represents the level of anisotropy of the tissue defined as the ratio ${}^{2}_{0}\lambda_{circ}/{}^{2}_{0}\lambda_{rad}$.

The stress-relaxation behavior of the tissue was also analyzed by calculating the initial slope ($\dot{T}^1$) and the saturated slope ($\dot{T}^2$) of the 900-second stress relaxation data. The initial slope of stress-relaxation was determined by using the first 5-second stress relaxation data, whereas the saturated slopes were considered as the stress relaxation between 500 seconds and 900 seconds (Fig. 1d). Here, the over-dot operator denotes the time derivative, i.e., $\dot{T} = dT/dt$.

2.4 Statistical analysis

To determine statistically significant differences in the mechanical responses of the paired fresh and frozen tissue samples, a nonparametric Mann-Whitney U test was performed using an in-house MATLAB (MathWorks, Natick, MA) program. This nonparametric test was chosen after analyses of the normality of the data using the quantile-quantile (Q-Q) plots, which showed that the data did not follow a normal distribution (Figs. S1–S2). Next, in our statistical analyses, the null hypothesis was that the difference in the mean between the control (fresh) tissue group and the frozen tissue group was equal to zero, meaning that the freezing storage had no statistically significant effect on the mechanics of the TVAL tissue sample. All quantities presented in this study are reported as mean ± standard error of the mean (SEM).

The quantities that were analyzed include data from biaxial mechanical testing (Fig. 1c): the peak tissue stretches ($^{2}_{0}\lambda_{circ}$ and $^{2}_{0}\lambda_{rad}$), the preconditioning stretches ($^{1}_{0}\lambda_{circ}$ and $^{1}_{0}\lambda_{rad}$), the mechanical stretches ($^{2}_{1}\lambda_{circ}$ and $^{2}_{1}\lambda_{rad}$), the elastic moduli at the high tension regime (E^{HT}_{circ} and E^{HT}_{rad}), the elastic moduli at the low tension regime (E^{LT}_{circ} and E^{LT}_{rad}), and the indices of extensibility (λ^{*}_{circ} and λ^{*}_{rad}). Quantities from biaxial stress relaxation testing were also analyzed (Fig. 1d): the percentage reductions in the membrane tensions, the time history of the membrane tensions ($T_{circ}(t)$ and $T_{rad}(t)$), the initial slopes of stress relaxation ($\dot{T}^{1}_{circ}$ and $\dot{T}^{1}_{rad}$), and the saturated slopes of stress relaxation ($\dot{T}^{2}_{circ}$ and $\dot{T}^{2}_{rad}$). Significance was considered as *statistically significant* ($p<0.05$), *nearly statistically significant* ($0.05\leq p<0.1$), and *statistically not significant* ($p\geq 0.1$).

3. Results

3.1 Thickness measurements

Measurements of the tissue thickness before and after freezing showed only a minimal change (<1%) in the tissue thickness: fresh TVAL, 0.35±0.04 mm; frozen TVAL, 0.35±0.04 mm. The thickness measurements and the effective testing edge lengths for all specimens are summarized in Table 1.

3.2 Biaxial mechanical testing results

The results from biaxial mechanical testing are summarized in Figures 2–4, the peak stretch values are summarized in Table 1, and the p-values from statistical comparisons are summarized in Table 2, which showed statistically insignificant differences in most parameters between the fresh and frozen tissue responses (Fig. 2a–c). Specifically, under equibiaxial loading (T_{circ}:T_{rad}=1:1), there was only a 3.4% difference observed in the circumferential peak stretch ($^{2}_{0}\lambda_{circ}$) between the fresh and frozen tissues (p=0.427) (Table 1). Similarly, the circumferential preconditioning stretch ($^{1}_{0}\lambda_{circ}$) had a 2.8% difference (p=0.308) (Fig, 3a), and the mechanical stretch ($^{2}_{1}\lambda_{circ}$) had a 0.6% difference (p=0.970) (Fig. 3b). As for the radial direction, similar trends were observed: $^{2}_{0}\lambda_{rad}$, 4.8% difference (p=0.791); $^{1}_{0}\lambda_{rad}$, 7.1% difference (p=0.241) (Fig. 3a); and $^{2}_{1}\lambda_{rad}$, 1.4% difference (p=0.734) (Fig. 3b). Values for the peak tissue stretches (Fig. 2b and Fig. 2c), the preconditioning stretches (Fig. 3c), and the mechanical stretches (Fig. 3d) associated with the other two biaxial loading protocols (T_{circ}:T_{rad}=0.5:1 and T_{circ}:T_{rad}=1:0.5) were comparable, and none demonstrated statistically significant differences.

In addition, the radial elastic modulus of the low-tension regime (E^{LT}_{rad}) was noted to be statistically significant or nearly statistically significant at each of the three loading ratios (Fig. 4b and Table 2). At the T_{circ}:T_{rad}=0.5:1 loading ratio, statistical significance was observed (p=0.038), whereas nearly statistical significance was observed under the loading protocols T_{circ}:T_{rad}=1:1 (p=0.054) and T_{circ}:T_{rad}=1:0.5 (p=0.089). As for the circumferential direction, E^{LT} was observed not to have a statistically significant difference (p=0.162). The

elastic modulus of the high-tension regime (E^{HT}) was not statistically significant in etiher tissue's direction: udner T_{circ}:T_{rad}=1:1 loading, the circumferential direction had a 6.1% difference (p=0.678) and the radial direction had a 17.8% difference (p=0.571). Other biaxial loading protocols had similar, statistically insignificant trends. The indices of extensibility (λ^*_{circ} and λ^*_{rad}) and the anisotropy index (AI) followed similarly statistically insignificant trends across the three loading protocols (Table 2), with the fresh TVAL tissues demonstrating slightly greater extensibility and a lessened material anisotropy than the frozen tissues.

3.3 Stress relaxation testing results

Analysis of the stress relaxation parameters showed mostly statistically insignificant differences, and these statistical analysis results are summarized in Table 3. For the initial slope ($\dot{T}^1$), there was a difference of 0.01 between the fresh and frozen tissues in the circumferential direction (p=0.909) and a difference of 0.04 in the radial direction (p=0.677). As for the saturated slope ($\dot{T}^2$), the differences between the fresh and frozen tissues were found to be 0.9×10^{-3} N/m in the circumferential direction (p=0.069) and 0.3×10^{-3} N/m in the radial direction (p=0.791) respectively.

4. Discussion

4.1 Overall findings

Comparison of the mechanical parameters between the fresh and the frozen TVAL showed minimal differences between the fresh and frozen tissues. Specifically, differences in the peak, preconditioning, and mechanical stretches between the two groups were statistically insignificant. Additionally, the elastic modulus of the high-tension regime and the index of extensibility were not significantly different. While the elastic modulus of the low-tension regime was found to have a statistically significant difference, this difference was only significant in the radial direction and was only nearly significant for most of the biaxial mechanical testing protocols. Finally, the analysis of the initial and saturated slopes of stress relaxation also showed no statistically significant differences. These findings suggest that freezing-based storage does not have a significant effect on the mechanical properties of the investigated atrioventricular heart valve leaflet tissue.

Although changes in the observed mechanical properties were statistically insignificant, the slight variations from the freezing storage observed in this study could impact the biaxial mechanical testing results of our previous studies (Jett *et al.*, 2018; Laurence *et al.*, 2019; Ross *et al.*, 2019). Specifically, the frozen tissues were found to be slightly stiffer and more anisotropic than the fresh tissues (Fig. 2), and the frozen tissues had a slightly lessened stress relaxation behavior than the fresh tissues (Fig. 5). This trend could have bearing on the tissue mechanics observed in previous studies of the AHV leaflets, and possibly obscure the results. For example, in another study performed by our lab, glycosaminoglycans (GAGs) were removed from previously-frozen AHV leaflets and the mechanical responses were characterized (Ross *et al.*, Under review). It was observed that the fully intact tissues were stiffer than tissues with a majority (>50%) of the GAGs removed, but part of this response

could be partially attributed to the freezing storage rather than the effect of the GAG removal. Overall, it is important to consider the method of tissue storage, when designing a study of soft biological materials such as atrioventricular heart valve leaflets. However, the effect of freezing on AHV leaflet mechanical properties was observed to be minimal, and our results suggest the mechanical responses of the tissues could be mostly preserved by freezing.

4.2 Study Limitations and Future Extensions

There are several limitations in this study. First, it is unknown whether the specimen size has a significant effect on the observed mechanical properties of the leaflets; however, preliminary investigations in our lab suggest this to have a minimal impact. There are also some limitations of our biaxial testing procedures, including: (i) the possibility for shear stress in the specimen using the tissue mounting hardware BioRake, while the shear deformations were found to be negligible if the tissue's directions were aligned with the primary axes of the biaxial testing system; and (ii) the stress relaxation procedure (15 minutes) was relatively short to capture the entire stress relaxation behavior of the TVAL tissue; however, it has been shown that the majority of relaxation occurs in the first 1000 seconds (Grashow *et al.*, 2006; Huang and Huang, 2015). There is also a potential limitation with the contact-based thickness measurement approach due to the possibility for slight tissue compression when performing the measurements. In our previous investigation we have shown reasonable agreement between our dial caliper-based approach and histological measurements (Jett *et al.*, 2018). Additionally, the exact freezing rate for the tissue specimen was unknown, acting as another potential limitation. Finally, the investigation on porcine heart valves may not automatically extend to the human heart valve leaflets and further research using human valves may need to be performed to fully evaluate the effect of freezing on human heart valves.

Future extensions of this study of the freezing effect include an examination of the effect of freezing over varied periods of time. In this study, tissues were frozen for 48 hours, but tissues have been frozen for a week or more before testing in the previous literature. Furthermore, freezing times may have varied from specimen-to-specimen with the assumption that there would be no effect on the observed mechanical behaviors. Although this experiment showed no significant changes due to freezing, longer storage times may show some effect in the quantified mechanical properties of the tissue. Additionally, the effects could be examined from varying freezing temperature, freezing methods, number of freeze-thaw cycles, or the freezing rates. Another future work could include analyzing the effect of freezer storage on the tissue microstructure, which may be linked to the differences in the observed mechanical properties such as the radial low-tension moduli. The effects of freezing storage on the mechanical properties of other atrioventricular valve leaflets not included in this study could also be investigated.

4.3 Conclusion

Our results from biaxial mechanical testing and stress relaxation testing of the tricuspid valve anterior leaflet suggested that the commonly adopted freezing storage procedure *does not significantly affect* the observed mechanical properties of the examined atrioventricular

heart valve leaflet. Most parameters from the testing did not demonstrate a significant difference between the fresh and frozen tissues. From this study, greater confidence can be had in the continued use of a freezing-based storage system for the preservation of AHV leaflet tissues.

The presented work has a broader impact to the field of AHV leaflet mechanical characterizations because it demonstrates the effect of a highly-employed storage method on the observed mechanical properties of the tissues. The finding that the storage method has minimal effect on the mechanics is useful as it provides a confirmation for those researchers that their reported mechanical parameters of the AHV leaflets are not skewed by their storage method. As an extension, this also reassures those researchers performing computational studies utilizing mechanical data from studies with a freezer-based leaflet storage method.

Supplementary Material

Refer to Web version on PubMed Central for supplementary material.

Acknowledgments

Support from the American Heart Association Scientist Development Grant (SDG) Award (16SDG27760143) is gratefully acknowledged. CHL was in part supported by the institutional start-up funds from the School of Aerospace and Mechanical Engineering (AME) and the research funding through the Faculty Investment Program from the Research Council at the University of Oklahoma (OU). CJ and GD were supported by the Mentored Research Fellowship (MRF) from the Office of Undergraduate Research and the Undergraduate Research Opportunity Program (UROP) sponsored by the VPR Office at OU. We also acknowledge undergraduate researchers Allyson Echols, Lauren Evans, Brennan Mullins, and Katherine Casey for their assistance with the biaxial mechanical testing.

References

Arzani A, Mofrad MRK, 2017. A strain-based finite element model for calcification progression in aortic valves. Journal of Biomechanics 65, 216–220. [PubMed: 29100595]

Ayoub S, Lee C-H, Driesbaugh KH, Anselmo W, Hughes CT, Ferrari G, Gorman RC, Gorman JH III, Sacks MS, 2017. Regulation of valve interstitial cell homeostasis by mechanical deformation: Implications for heart valve disease and surgical repair. Journal of the Royal Society Interface 14, 20170580.

Changoor A, Fereydoonzad L, Yaroshinsky A, Buschmann MD, 2010. Effects of refrigeration and freezing on the electromechanical and biomechanical properties of articular cartilage. Journal of biomechanical engineering 132, 064502. [PubMed: 20887036]

Clavert P, Kempf J-F, Bonnomet F, Boutemy P, Marcelin L, Kahn J-L, 2001. Effects of freezing/thawing on the biomechanical properties of human tendons. Surgical and Radiologic Anatomy 23, 259–262. [PubMed: 11694971]

Delgadillo JOV, Delorme S, El-Ayoubi R, DiRaddo R, Hatzikiriakos SG, 2010. Effect of freezing on the passive mechanical properties of arterial samples. Journal of Biomedical Science and Engineering 3, 645.

Eckert CE, Fan R, Mikulis B, Barron M, Carruthers CA, Friebe VM, Vyavahare NR, Sacks MS, 2013. On the biomechanical role of glycosaminoglycans in the aortic heart valve leaflet. Acta Biomaterialia 9, 4653–4660. [PubMed: 23036945]

Foutz TL, Stone EA, Abrams CF III, 1992. Effects of freezing on mechanical properties of rat skin. American Journal of Veterinary Research 53, 788–792. [PubMed: 1524309]

Giannini S, Buda R, Di Caprio F, Agati P, Bigi A, De Pasquale V, Ruggeri A, 2008. Effects of freezing on the biomechanical and structural properties of human posterior tibial tendons. International orthopaedics 32, 145–151. [PubMed: 17216243]

Grashow JS, Sacks MS, Liao J, Yoganathan AP, 2006. Planar biaxial creep and stress relaxation of the mitral valve anterior leaflet. Annals of Biomedical Engineering 34, 1509–1518. [PubMed: 17016761]

Huang H-YS, Balhouse BN, Huang S, 2012. Application of simple biomechanical and biochemical tests to heart valve leaflets: implications for heart valve characterization and tissue engineering. Proceedings of the Institution of Mechanical Engineers. Part H: Journal of Engineering in Medicine 226, 868–876.

Huang S, Huang H-YS, 2015. Biaxial stress relaxation of semilunar heart valve leaflets during simulated collagen catabolism: Effects of collagenase concentration and equibiaxial strain state. Proceedings of the Institution of Mechanical Engineers, Part H: Journal of Engineering in Medicine 229, 721–731.

Jett S, Laurence D, Kunkel R, Babu AR, Kramer K, Baumwart R, Towner R, Wu Y, Lee C-H, 2018. An investigation of the anisotropic mechanical properties and anatomical structure of porcine atrioventricular heart valves. J. Mech. Behav. Biomed. Mater 87, 155–171. [PubMed: 30071486]

Kaye B, Randall C, Walsh D, Hansma P, 2012. The effects of freezing on the mechanical properties of bone. The Open Bone Journal 4.

Khoiy KA, Amini R, 2016. On the biaxial mechanical response of porcine tricuspid valve leaflets. Journal of Biomechanical Engineering 138, 104504-104504-104506.

Kidane AG, Burriesci G, Cornejo P, Dooley A, Sarkar S, Bonhoeffer P, Edirisinghe M, Seifalian AM, 2009. Current developments and future prospects for heart valve replacement therapy. Journal of Biomedical Materials Research Part B: Applied Biomaterials 88B, 290–303.

Kunzelman KS, Reimink MS, Cochran RP, 1997. Annular dilatation increases stress in the mitral valve and delays coaptation: A finite element computer model. Cardiovascular Surgery 5, 427–434. [PubMed: 9350801]

Laurence D, Ross C, Jett S, Johns C, Echols A, Baumwart R, Towner R, Liao J, Bajona P, Wu Y, Lee C-H, 2019. An investigation of regional variations in the biaxial mechanical properties and stress relaxation behaviors of porcine atrioventricular heart valve leaflets. J. Biomech 83, 16–27. [PubMed: 30497683]

Lee C-H, Rabbah J-P, Yoganathan AP, Gorman RC, Gorman JH III, Sacks MS, 2015. On the effects of leaflet microstructure and constitutive model on the closing behavior of the mitral valve. Biomechanics and Modeling in Mechanobiology 14, 1281–1302. [PubMed: 25947879]

Liao J, Yang L, Grashow J, Sacks MS, 2007. The relation between collagen fibril kinematics and mechanical properties in the mitral valve anterior leaflet. Journal of Biomechanical Engineering 129, 78–87. [PubMed: 17227101]

Linde F, Sørensen HCF, 1993. The effect of different storage methods on the mechanical properties of trabecular bone. Journal of biomechanics 26, 1249–1252. [PubMed: 8253829]

Matthews LS, Ellis D, 1968. Viscoelastic properties of cat tendon: effects of time after death and preservation by freezing. Journal of biomechanics 1, 65–71. [PubMed: 16329293]

May-Newman K, Yin FC, 1995. Biaxial mechanical behavior of excised porcine mitral valve leaflets. Am. J. Physiol. Heart Circ. Physiol 269, H1319–H1327.

O'Leary SA, Doyle BJ, McGloughlin TM, 2014. The impact of long term freezing on the mechanical properties of porcine aortic tissue. Journal of the mechanical behavior of biomedical materials 37, 165–173. [PubMed: 24922621]

Pant AD, Thomas VS, Black AL, Verba T, Lesicko JG, Amini R, 2018. Pressure-induced microstructural changes in porcine tricuspid valve leaflets. Acta Biomaterialia 67, 248–258. [PubMed: 29199067]

Pelker RR, Friedlaender GE, Markham TC, Panjabi MM, Moen CJ, 1983. Effects of freezing and freeze-drying on the biomechanical properties of rat bone. Journal of Orthopaedic Research 1, 405–411.

Pham T, Sulejmani F, Shin E, Wang D, Sun W, 2017. Quantification and comparison of the mechanical properties of four human cardiac valves. Acta Biomaterialia 54, 345–355. [PubMed: 28336153]

Pham T, Sun W, 2014. Material properties of aged human mitral valve leaflets. Journal of Biomedical Materials Research, Part A 102, 2692–2703. [PubMed: 24039052]

Pokutta-Paskaleva A, Sulejmani F, DelRocini M, Sun W, 2019. Comparative mechanical, morphological, and microstructural characterization of porcine mitral and tricuspid leaflets and chordae tendineae. Acta Biomaterialia 85, 241–252. [PubMed: 30579963]

Reddy JN, 2013. An Introduction to Continuum Mechanics. Cambridge University Press.

Rogers JH, Bolling SF, 2009. The tricuspid valve: Current perspective and evolving management of tricuspid regurgitation. Circulation 119, 2718–2725. [PubMed: 19470900]

Ross C, Laurence D, Richardson J, Babu A, Evans L, Beyer E, Wu Y, Towner R, Fung K-M, Mir A, Burkhart HM, Holzapfel GA, Lee C-H, Under review. An investigation of the glycosaminoglycan contribution to biaxial mechanical behaviors of porcine atrioventricular heart valve leaflets. J R Soc Interface.

Ross C, Laurence D, Wu Y, Lee C-H, 2019. Biaxial mechanical characterizations of atrioventricular heart valves. J. Vis. Exp 146, e59170.

Sacks MS, 2000. Biaxial mechanical evaluation of planar biological materials. Journal of Elasticity 61, 199.

Santago A, Kemper A, McNally C, Sparks J, Duma S, 2009. Freezing affects the mechanical properties of bovine liver. Biomed. Sci. Instrum 45, 24–29. [PubMed: 19369734]

Smith C, Young I, Kearney J, 1996. Mechanical properties of tendons: changes with sterilization and preservation. Journal of biomechanical engineering 118, 56–61. [PubMed: 8833075]

Stella JA, Liao J, Sacks MS, 2007. Time-dependent biaxial mechanical behavior of the aortic heart valve leaflet. Journal of Biomechanics 40, 3169–3177. [PubMed: 17570376]

Stella JA, Sacks MS, 2007. On the biaxial mechanical properties of the layers of the aortic valve leaflet. Journal of Biomechanical Engineering 129, 757–766. [PubMed: 17887902]

Stemper BD, Yoganandan N, Stineman MR, Gennarelli TA, Baisden JL, Pintar FA, 2007. Mechanics of fresh, refrigerated, and frozen arterial tissue. Journal of Surgical Research 139, 236–242.

Sun W, Martin C, Pham T, 2014. Computational modeling of cardiac valve function and intervention. Annual Review of Biomedical Engineering 16, 53–76.

Tadmor EB, Miller RE, Elliott RS, 2012. Continuum Mechanics and Thermodynamics: From Fundamental Concepts to Governing Equations. Cambridge University Press.

Venkatasubramanian RT, Grassl ED, Barocas VH, Lafontaine D, Bischof JC, 2006. Effects of freezing and cryopreservation on the mechanical properties of arteries. Annals of Biomedical engineering 34, 823–832. [PubMed: 16619131]

Waller BF, Howard J, Fess S, 1994. Pathology of mitral valve stenosis and pure mitral regurgitation—Part I. Clinical Cardiology 17, 330–336. [PubMed: 8070151]

Waller BF, Howard J, Fess S, 1995. Pathology of tricuspid valve stenosis and pure tricuspid regurgitation—Part I. Clinical Cardiology 18, 97–102. [PubMed: 7720297]

Wells SM, Pierlot CM, Moeller AD, 2012. Physiological remodeling of the mitral valve during pregnancy. American Journal of Physiology-Heart and Circulatory Physiology.

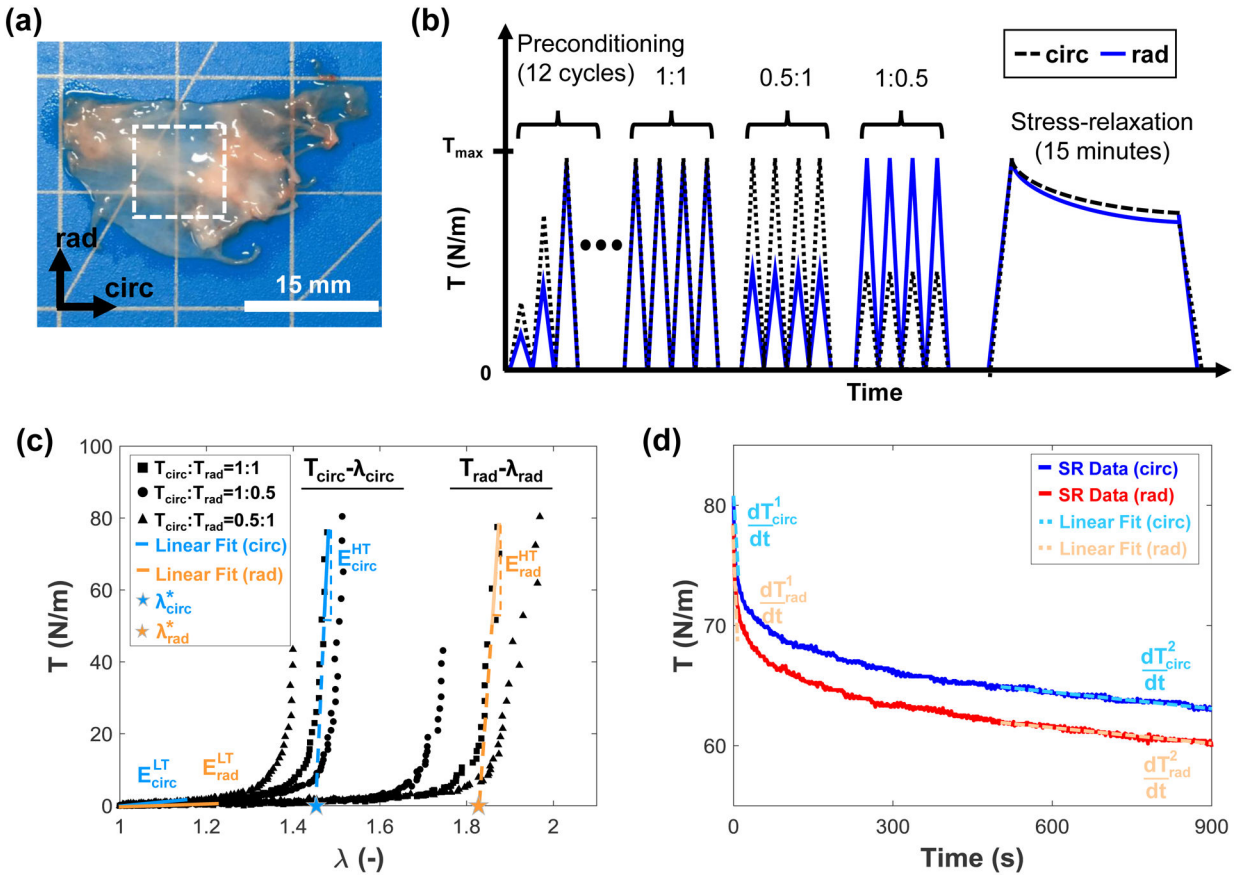

Figure 1 –.

(a) The tricuspid valve anterior leaflet was excised and sectioned into a central 10mm × 10mm region before (b) biaxial mechanical testing involving a preconditioning protocol, biaxial loading to ratios of the peak membrane tension (T_{circ}:T_{rad}=1:1, 1:0.5, 0.5:1), and stress-relaxation testing. (c) Parameters analyzed from the biaxial loading include the index of extensibility (λ*), tangent modulus at the low-tension (E^{LT}) and high-tension regimes (E^{HT}), and the stretches (λ). (d) Parameters analyzed from the stress relaxation include the membrane tension decay, and the initial and saturated membrane tension rates of change ($\dot{T}^{1}$ and $\dot{T}^{2}$, respectively).

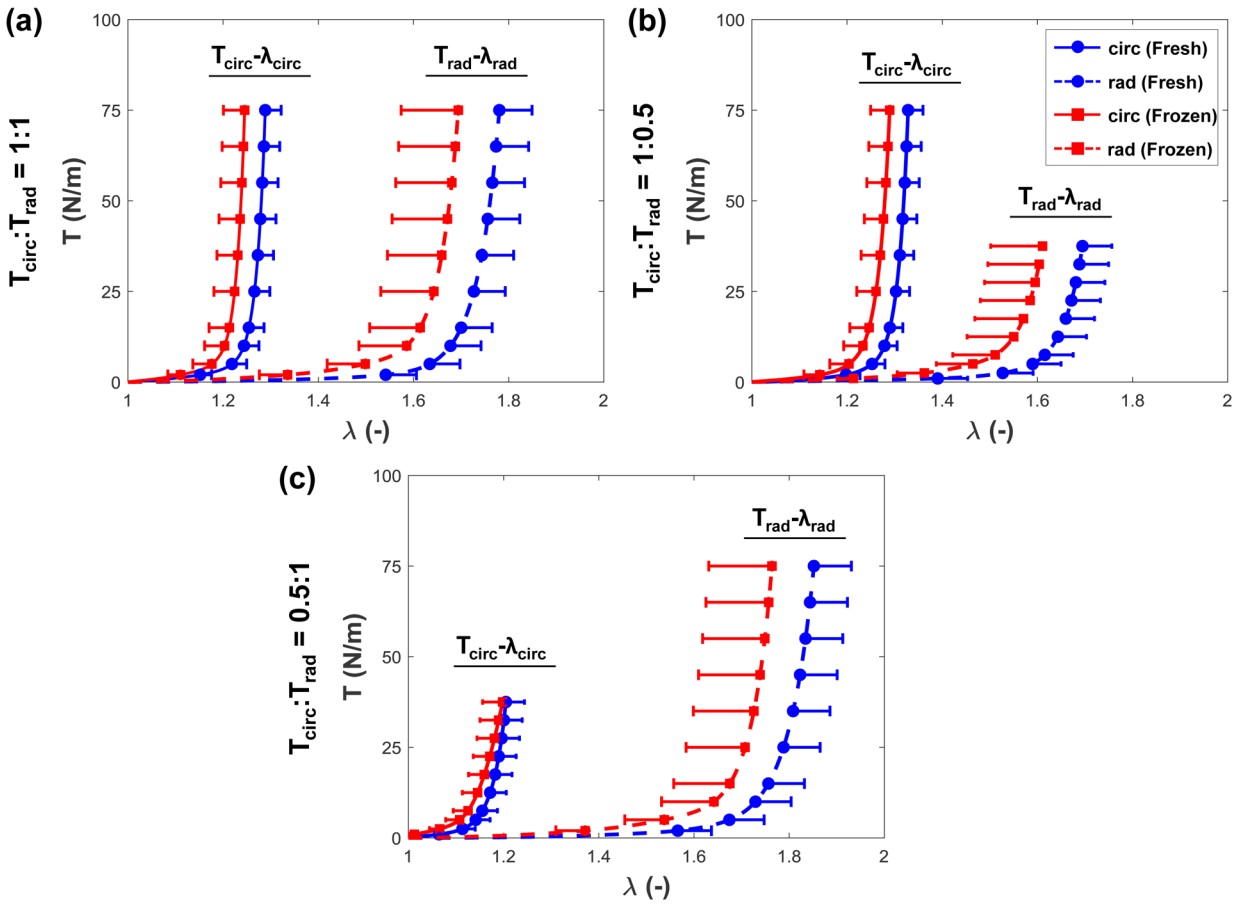

Figure 2 –.

Peak stretches (λ_0^2) of the fresh and frozen tricuspid valve anterior leaflet tissues under the (a) T_{circ}:T_{rad}=1:1, (b) T_{circ}:T_{rad}=1:0.5, and (c) T_{circ}:T_{rad}=0.5:1 loading ratios.

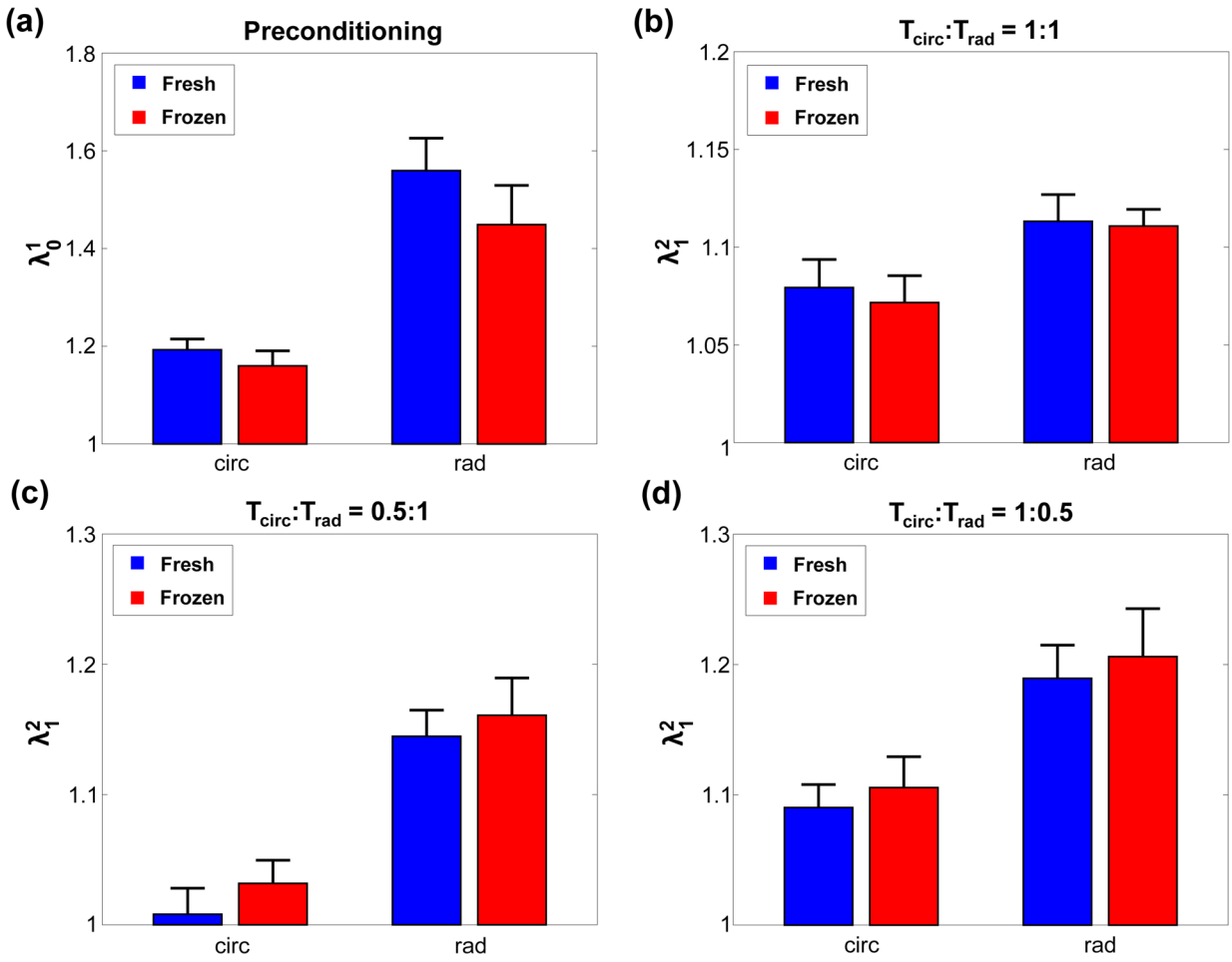

Figure 3 –.

(a) Preconditioning stretches ($^1_0\lambda$), and mechanical stretches ($^2_1\lambda$) at the 3 biaxial loading protocols: (b) T_{circ}:T_{rad}=1:1, (c) T_{circ}:T_{rad}=1:0.5, and (d) T_{circ}:T_{rad}=0.5:1 for the fresh and frozen tricuspid valve anterior leaflet tissues.

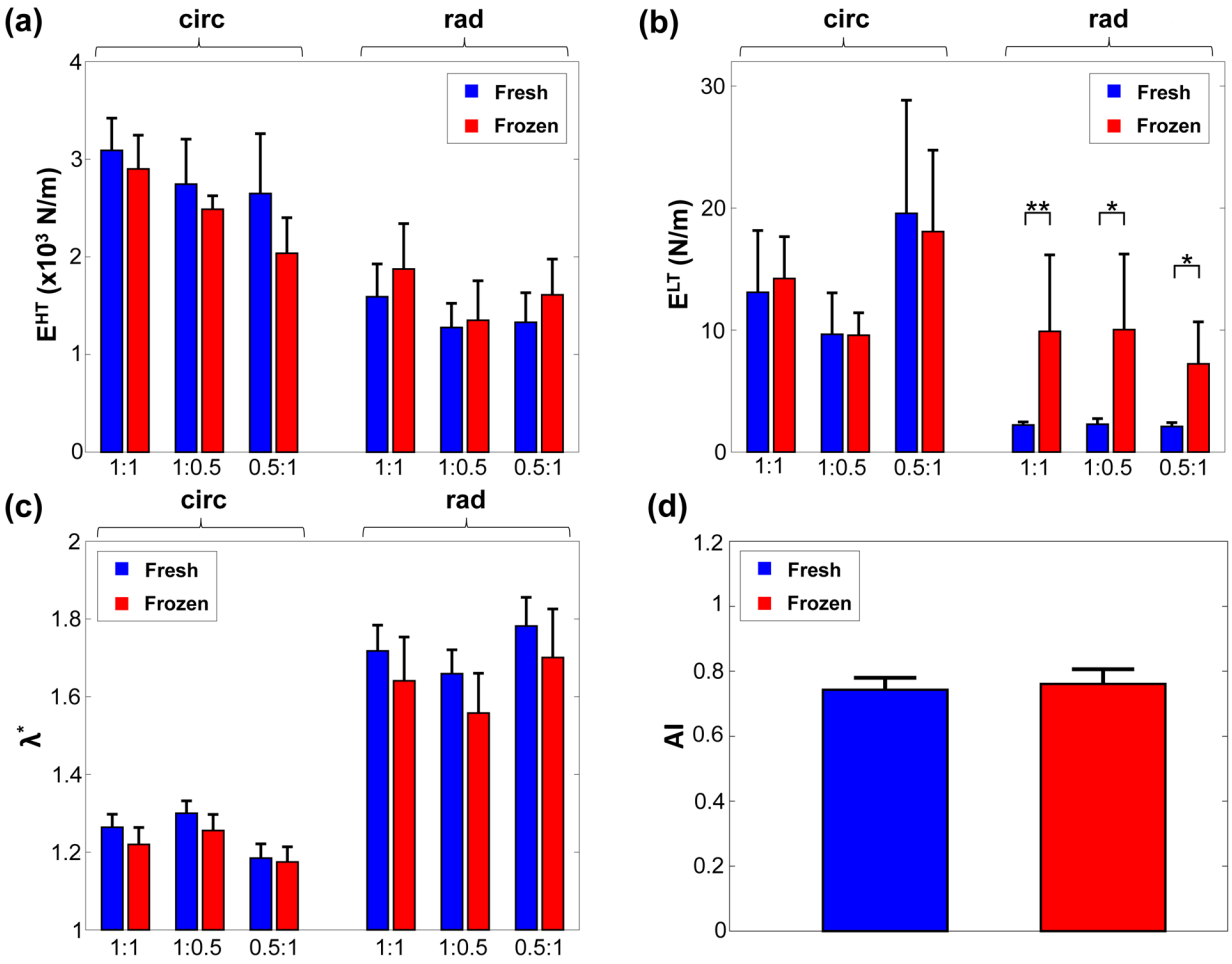

Figure 4 –.

Comparison of the (a) low-tension modulus (E^{LT}), (b) high-tension modulus (E^{HT}), (c) index of extensibility (λ^*), and (d) anisotropy indices (AI) between the fresh and frozen tissues under 3 different biaxial loading protocols. *, statistically significant ($p<0.05$); **, nearly statistically significant ($0.05 \leq p < 0.1$).

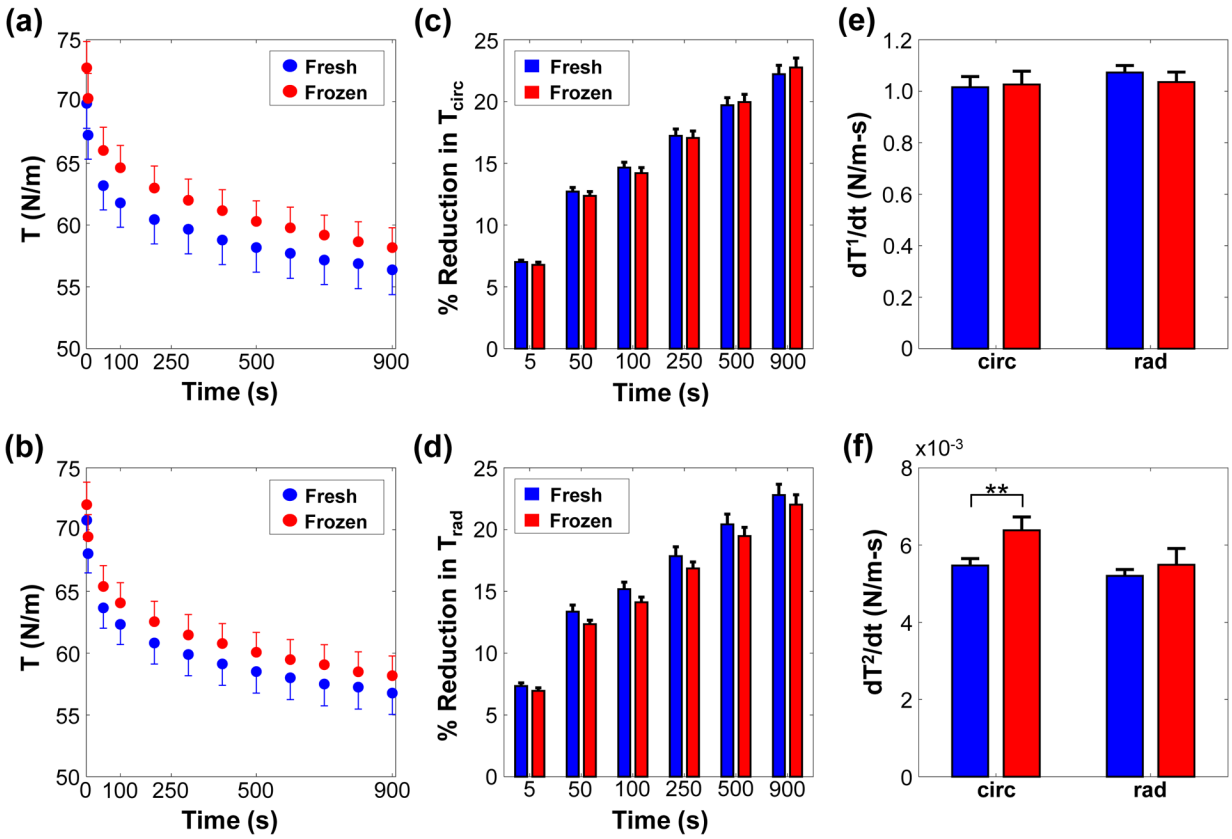

Figure 5 –.

The stress-relaxation of the fresh and frozen tricuspid valve anterior leaflet in the (a) circumferential and (b) radial directions, the percent reduction of the stress-relaxation in the (c) circumferential and (d) radial directions, and the (e) initial ($\dot{T}^1$) and (f) saturated ($\dot{T}^2$) slopes of the stress-relaxation reduction behavior. **, nearly statistically significant ($0.05 \leq p < 0.1$).

Table 1 –

Tissue thickness, effective edge length, and peak stretches for all the investigated TVAL tissue specimens.

TVAL Specimen ID	Fresh (Control)				Frozen			
	Thickness (mm)	Effective Edge Length (mm)	$^{2}_{0}\lambda_{circ}$	$^{2}_{0}\lambda_{rad}$	Thickness (mm)	Effective Edge Length (mm)	$^{2}_{0}\lambda_{circ}$	$^{2}_{0}\lambda_{rad}$
1	0.30	7.5	1.17	1.81	0.25	6.0	1.20	2.21
2	0.18	6.5	1.15	1.58	0.35	6.0	1.14	1.19
3	0.16	8.5	1.45	1.64	0.19	7.0	1.05	1.09
4	0.47	8.5	1.40	1.80	0.47	7.0	1.18	1.49
5	0.40	8.5	1.33	1.34	0.31	7.0	1.36	1.54
6	0.30	8.5	1.37	2.10	0.35	7.0	1.47	1.87
7	0.32	8.5	1.20	1.80	0.30	7.0	1.19	1.65
8	0.51	7.5	1.34	2.01	0.53	6.5	1.30	1.84
9	0.41	8.0	1.18	1.87	0.49	7.0	1.12	1.86
10	0.48	8.5	1.29	1.86	0.20	7.0	1.44	2.20
Mean	0.35	8.1	1.29	1.78	0.35	6.8	1.25	1.69
SEM	0.04	0.2	0.03	0.07	0.04	0.1	0.05	0.12

Table 2 –

p-values from the statistical comparison of the quantities between the control (C) and frozen (F) TVAL tissue specimens (n=10). All values are reported as mean ± SEM.

Loading	Quantity		*p*-value (Fresh vs. Frozen)
Preconditioning	$\overset{1}{0}\lambda$	circ	0.308
		rad	0.241
T_{circ}:T_{rad}=1:1	$\overset{2}{0}\lambda$	circ	0.427
		rad	0.791
	$\overset{2}{1}\lambda$	circ	0.969
		rad	0.734
	E^{HT} (N/m)	circ	0.678
		rad	0.571
	E^{LT} (N/m)	circ	0.162
		rad	0.054 *
	λ^*	circ	0.473
		rad	0.678
	AI		0.570
T_{circ}:T_{rad}=0.5:1	$\overset{2}{0}\lambda$	circ	0.909
		rad	0.678
	$\overset{2}{1}\lambda$	circ	0.427
		rad	0.791
	E^{HT} (N/m)	circ	0.791
		rad	0.571
	E^{LT} (N/m)	circ	0.186
		rad	0.038 *
	λ^*	circ	0.791
		rad	0.623
T_{circ}:T_{rad}=1:0.5	$\overset{2}{0}\lambda$	circ	0.345
		rad	0.521
	$\overset{2}{1}\lambda$	circ	0.850
		rad	0.850
	E^{HT} (N/m)	circ	0.623
		rad	0.678
	E^{LT} (N/m)	circ	0.308
		rad	0.089 *
	λ^*	circ	0.385
		rad	0.385

*: statistically significant ($p<0.05$)

**: nearly statistically significant ($0.05\leq p<0.1$)

Table 3 –

Comparison of the stress-relaxation parameters between the control (C) and frozen (F) TVAL tissue samples (n=10). All values are reported as mean ± SEM.

Quantity		Fresh (Control)	Frozen	*p*-value
$\dot{T}^1$ (N/m)	circ	1.01 ± 0.04	1.02 ± 0.05	0.909
	rad	1.07 ± 0.02	1.03 ± 0.03	0.677
$\dot{T}^2$ (x10^{-3} N/m)	circ	5.50 ± 0.20	6.40 ± 0.30	0.069**
	rad	5.20 ± 0.20	5.50 ± 0.40	0.791

**: nearly statistically significant (0.05≤p<0.1)